Effects of diamagnetic levitation on bacterial growth in liquid

Richard J. A. Hill[*,1], Oliver J. Larkin[2], Paul Anthony[2], Michael R. Davey[2], Laurence Eaves[1], Catherine E. D. Rees[2], Camelia E. Dijkstra[2]

[1] School of Physics and Astronomy, University of Nottingham, Nottingham, NG7 2RD, UK.
[2] School of Biosciences, University of Nottingham, Sutton Bonington Campus, Loughborough, LE12 5RD, UK.

* email: richard.hill@nottingham.ac.uk.

Diamagnetic levitation is a technique that uses a strong, spatially-varying magnetic field to levitate diamagnetic materials, such as water and biological cells. This technique has the potential to simulate aspects of weightlessness, on the Earth. In common with all ground-based techniques to simulate weightlessness, however, there are effects introduced by diamagnetic levitation that are not present in space. Since there have been few studies that systematically investigate these differences, diamagnetic levitation is not yet being fully exploited. For the first time, we critically assess the effect of diamagnetic levitation on a bacterial culture in liquid. We used a superconducting magnet to levitate growing bacterial cultures for up to 18 hours, in a series of experiments to determine the effect of diamagnetic levitation on all phases of the bacterial growth cycle. We find that diamagnetic levitation increases the rate of population growth in a liquid culture. The speed of sedimentation of the bacterial cells to the bottom of the container is considerably reduced. Further experiments and microarray gene analysis show that the growth enhancement is due to greater oxygen availability in the magnetically levitated sample. We demonstrate that the magnetic field that levitates the cells also induces convective stirring in the liquid, an effect not present in microgravity. We present a simple theoretical model, showing how the paramagnetic force on dissolved oxygen can cause the liquid to become unstable to convection when the consumption of oxygen by the bacteria generates an oxygen concentration gradient. We propose that this convection enhances oxygen availability by transporting oxygen around the sample. Since convection is absent in space, these results are of significant importance and timeliness to researchers considering using

diamagnetic levitation to explore weightless effects on living organisms and a broad range of other topics in the physical and life sciences.

It is important to understand how weightlessness influences bacterial behavior, not only for the health of astronauts, but also for the long-term future of space exploration (Cogoli 2006). Earth-based techniques can simulate aspects of a microgravity environment, but are either time-limited to a few seconds or minutes (drop towers, parabolic flights and sounding rockets), or use rotation, which can introduce artifacts due to the rotating reference frame (clinostats, random positioning machine) (van Loon 2007).

Here, we use the diamagnetic force induced by a strong spatially-varying magnetic field to balance the force of gravity (Beaugnon 1991, Beaugnon 2001, Simon & Geim 2000). Just as the centrifugal force balances the gravitational force on an orbiting spacecraft, we use the diamagnetic force to oppose the force of gravity on a levitating object. The potential of diamagnetic levitation as a laboratory-based tool to study the effects of weightlessness on living organisms was first demonstrated by Berry and Geim (1997) who levitated a living frog using a Bitter (resistive) magnet. By using a superconducting magnet capable of levitating water (Hill & Eaves 2008), it is possible to levitate biological samples for several weeks, or even months, allowing effects on growth and behavior to be investigated (Qian 2009). Guevorkian and Valles (2006) reported that *Paramecia* change their swimming behavior in magnetically-altered effective gravity, in response to the altered buoyancy of the cells. Coleman *et al*. (2007) investigated the effect of magnetic levitation on growth and cell cycle changes in wild type yeast cells, concluding that neither the growth nor the cell cycle was affected by the magnetic field when cells were levitated, but that growth was reduced at increased effective gravity. However, some selective effects were seen on cells with specific mutation in transcription factors, known to mediate responses to environmental stresses such as gravity and shear stress, indicating that adaptive gene expression was required for the cells to be able to grow normally. Our previous experiments on magnetically levitated *Arabidopsis thaliana* cell cultures have also shown that adaptive responses occur, again detected by changes in the expression of transcription factors. In this case, the adaptations were similar to those seen when cells experienced simulated weightlessness in a random positioning machine (Babbick 2007). Wilson et al. (2007) have also shown that space flight alters bacterial gene expression and virulence, in this case due to a decrease in the levels of the global gene

regulator Hfq, again indicating the need for adaptation to growth in a weightless environment.

Here we show that diamagnetic levitation increases the rate of population growth and final cell density of bacteria in a liquid culture, and investigate the mechanism leading to this enhancement. It is often assumed that in a magnetic field capable of diamagnetically levitating water, biological samples will experience pseudo-weightless conditions, by virtue of their large water content. We test these assumptions theoretically and experimentally.

For these experiments, *Escherichia coli* and *Staphylococcus epidermidis* were chosen as examples of human commensal bacteria, and as representatives of the Gram-negative and Gram-positive groups, respectively. We use a 17 Tesla superconducting solenoid with a 5 cm-diameter, temperature-controlled bore to levitate bacterial cultures in nutrient broth. Within the bore, the diamagnetic culture medium and bacteria are repelled from the region of maximum magnetic field at the center of the solenoid. The vertical component of the diamagnetic force on an object with volume V in the magnetic field B is given by $F_{mag} = \chi VBB'/\mu_0$ (Simon & Geim 2000) where $B' = dB/dz$ is the vertical component of the field-gradient, χ is volume magnetic susceptibility and $\mu_0 = 4\pi\times10^{-7}$ NA^{-2}. For levitation, we require the magnetic force to balance the object's weight, ρVg, where $g = 9.8$ ms^{-2} and ρ is the object's density. We define the *effective gravity* Γ such that the net force on the object in the magnetic field is given by $F = (F_{mag} - \rho Vg) = -\rho V\Gamma$ (note that, in this definition, a net *downward* force F is indicated by a *positive* value of Γ). Hence, when the culture medium (which is composed mostly of water) is levitating, we have $\Gamma = g - \chi_w BB'/\rho_w\mu_0 = 0$, where $\chi_w = -9\times10^{-6}$ and $\rho_w = 1000$ kg m^{-3} are the magnetic volume susceptibility (in S.I. units) and density of water respectively. This condition is satisfied approximately 80 mm above the center of our solenoid, where $BB' = -1370$ T^2 m^{-1} ($B = 12.5$ T).

Whether an individual cell floats or sinks in the culture medium depends on the difference between the cell's weight and the weight of fluid displaced by the cell. In space, e.g. in an orbiting spacecraft, both weights are zero, so the cells are neutrally buoyant. The difference between the (vertical component of the) buoyancy force and the cell weight is $\Delta F = (\chi_c - \chi_w)VBB'/\mu_0 - (\rho_c - \rho_w)Vg$ (Catherall 2005), where χ_c is the (spatially-averaged) volume magnetic susceptibility of the cell, V is the cell volume and ρ_c is the buoyant density of the cell (i.e. its mass divided by V). For neutral buoyancy, we require the net force acting on the

cell to be zero; that is, we require $\Gamma_c = g - \Delta\chi BB'/\Delta\rho\mu_0 = 0$, where $\Delta\chi = \chi_c - \chi_w$, $\Delta\rho = \rho_c - \rho_w$. Since the buoyant density of the bacterial cells is $\rho_c \approx 1090$ kg m^{-3} (Kubitschek 1986), we expect the cells to sediment in the culture medium, outside the magnet. We now consider whether the diamagnetic force on the cells and the fluid can prevent the cells from sinking. We estimate $\Delta\chi \approx -(8 \pm 3)\times10^{-7}$ experimentally by measuring the levitation position in the bore (Tanimoto 2005); most of the experimental error in this measurement is due to uncertainty in the water content of the bacterial pellet. From this result, we estimate that $\Gamma_c = (0.0 \pm 0.3)g$ at the levitation point of the culture medium (where $\Gamma = 0g$). This analysis suggests that it *is* possible to achieve a pseudo-weightless condition in the magnetically levitated bacterial culture, in the sense that the fluid medium is weightless ($\Gamma = 0$) and the cells are *simultaneously* neutrally buoyant in the fluid ($\Gamma_c \approx 0g$). We test this hypothesis experimentally. Note that, off the axis of the solenoid, the effective gravity *vector* is given by $\mathbf{\Gamma} = \chi_w B\nabla B/\rho_w\mu_0 - g\mathbf{k}$, where $\mathbf{k}$ is a unit vector pointing vertically upward. Close to the stable equilibrium levitation point, $\mathbf{\Gamma}$ points radially inward toward the levitation point; $|\mathbf{\Gamma}|\sim0.1g$ approximately 10 mm from the levitation point. Fig. S1 shows the magnitude and direction of $\mathbf{\Gamma}$ within the culture.

We use culture volumes V >1 ml to allow for sampling during the experiment and to ensure that the culture is not significantly affected by evaporation. Strong magnetic fields of the order $B \sim 10$ T are required to magnetically levitate culture volumes of this size; in our experiments, $B \approx 12.5$ T at the levitation point. There is evidence that B fields of this strength affect biological organisms at the cellular level. For example, striking changes were observed in the orientation of cell-division cleavage planes in developing frogs eggs in a static field $B \sim 1$ T (Denegre 1998). The magnetic field can affect cells through stresses arising from the differences in χ and ρ between cell structures, or magnetic torques arising from anisotropy in χ (see, for example, Hill 2007). The first of these forces requires a magnetic field gradient, whereas a torque can arise in a homogeneous magnetic field. The significance of internal stresses and torques depends on whether the energy associated with such forces is larger than the thermal energy scale. A third possibility is that the magnetic field can affect biochemical kinetics (Steiner 1989). We shall not consider these possibilities in further detail here. However, by using a control sample placed at the center of the solenoid coil, where $\Gamma \approx 1g$ and $B \approx 16.3$ T, we can distinguish *experimentally* between the effects of magnetic forces proportional to the field gradient dB/dz and magnetic effects that do not depend on a field

gradient. As an additional control, samples were also placed below the center of the solenoid, where $\Gamma \approx 2g$ (i.e. where gravity and the magnetic force are additive) and $B \approx 12.5$ T. We label the sample at the levitation point "0*g**", and label the two controls "1*g**" and "2*g**" corresponding to the effective gravity in each position; the asterisk on the label indicates the sample is in a magnetic field. We use the label "1*g*" to indicate the control sample, grown outside the magnet.

To test our hypothesis that sedimentation of the bacteria in the culture is inhibited when the culture medium is levitated, we used *E. coli* transformed to a green fluorescence phenotype to visualize the distribution of cells within the culture vessel. Cultures were exposed to the magnetic field, one at each of the positions 0*g**, 1*g** and 2*g**, simultaneously at a temperature of 37 °C for 18 h. Figure 1 shows that the sedimentation rate of cells was significantly reduced in the 0*g** position, compared to the 1*g** sample, indicated by the significantly greater optical density of the culture throughout the tube. At the 1g* position, some cells remained in suspension, but the density of the suspended culture was clearly less than the 0g* sample and cells were concentrated at the bottom of the liquid. Sedimentation at the 2*g** position was enhanced compared to the 1*g** sample: the supernatant was almost clear, with the cells forming a layer on the bottom of the vessel.

To investigate the effect of levitation on the growth of these cultures, cell density was measured as a function of time by taking optical density (OD_{600nm}) measurements at approximately 1 h intervals to determine growth rate and lag time. Cultures of untransformed *E. coli* and *S. epidermidis* were grown within the magnet at the three different positions (0*g**, 1*g** and 2*g**). In addition, control samples were incubated outside the magnet (1*g*). Cultures within the magnet bore and the 1*g* control sample were incubated statically at 37 °C. Each sample was mixed prior to measurement. Figure 2 shows that for both *E. coli* and *S. epidermidis* cultures grown at 0*g**, an overall enhancement of growth was apparent compared to the static (1*g*) control cultures. No difference in the lag phase or initial growth rate was observed when cultures had low cell density. However, the cultures at 1*g** and 2*g** and the 1*g* control all showed a lower initial growth rate than the 0*g** cultures (Fig. 2). The final cell density in the 0g* samples was approximately 1.5 times that of the control cultures. These results are reproducible and statistically significant. The growth in the 1g control is comparable to that in the 1g* sample, demonstrating that, in the absence of a magnetic field gradient, the magnetic field has no observable effect on the growth. For comparison, we

performed an experiment on a *shaken* culture outside the magnet, in which we expect the liquid to be fully aerated. We found that, although growth was enhanced at 0*g** compared to all the *static* cultures, it was not as high as that achieved by the aerated culture outside the magnet (Tables 1a and b). Liquid loss via evaporation was insignificant because the cultures vessels were air tight.

One possible reason that the growth rate is quicker in the shaken, aerated culture is that availability of O_2 is rate-limiting in the static cultures. To test this experimentally, we performed experiments in tubes of different cross-sectional area *A*, containing different volumes of medium *V*. We found a clear positive relationship between final cell mass and *A*/*V* (Fig. 3). This result lends weight to the hypothesis that the availability of O_2 is rate-limiting in these experiments, since the O_2 flux across the air/water interface is proportional to *A* and the O_2 concentration of the liquid resulting from this flux is inversely proportional to *V*. To confirm that availability of O_2 is rate-limiting, cultures were oxygenated from the bottom of the vessel by using the artificial gas carrier perfluorodecalin (PFC). PFC has a high saturation capacity for O_2, and is both more dense than, and immiscible with, water; it forms a discrete layer at the bottom of the culture and has been shown previously to enhance growth of bacterial cultures (Atlung 1997). All the samples with PFC showed enhanced growth compared to samples without PFC. Significantly, under these conditions, the final cell mass of the 0*g** sample was as high as the aerated cultures, and the 1*g**, 2*g** and 1*g* cultures all grew as well as the 0*g** sample without PFC (Tables 1a and b), confirming that O_2 is limiting in the lower region of the static cultures. This result suggests that magnetic levitation increases the availability of O_2. We discuss the possible mechanism shortly.

In adapting to different growth conditions, *E. coli* alters the composition of its respiratory pathways, changing the amount of different terminal oxidases to optimize its respiratory chain according to the substrates present and the physiological needs of the cell. Cytochrome b_o, encoded by the *cyoABCDE* operon, operates at high oxygen concentration and has low affinity for oxygen. Expression of the *cyo* operon is decreased under anaerobic conditions by the global anaerobic regulators ArcA and Fnr (Cotter 1992). The AppB cytochrome bd-type oxidase has a high oxygen affinity and is encoded in an operon with AppA (pH 2.5 acid phosphatase). Their expression is regulated by AppY and stress-response sigma factor RpoS under microaerobic conditions, when AppB may be required for efficient electron transport (Atlung 1997). We used microarray-based gene expression profiling to

investigate the response to O_2 depletion. RNA was extracted from each of the *E. coli* cultures grown under the different test conditions when the cells reached mid-exponential growth phase (OD_{600nm}= 0.5) and samples analyzed on an *E. coli* oligonucleotide array (Table 2). Expression of genes in the *cyo* operon were consistently ~2-fold up-regulated in the 0*g** samples compared to all other static samples. No significant difference in expression of these genes was detected between the 0*g** and the aerated culture. The opposite pattern was seen for genes in the *app* operon; the expression of these genes was enhanced at 2*g** which we predict to be the most anaerobic condition. Additionally, the anaerobic growth regulator *fnr* was down-regulated in the 0*g** compared to 2*g** sample. In general, genes known to be associated with anaerobic adaptation were more highly expressed in samples with the lowest growth. Changes in expression of *cyoA* and *appB* were also confirmed by real-time RT-PCR analysis and showed that the expression of the *cyoA* gene was enhanced at 0*g** compared with the control (Table 3), with the 1.5-fold change observed being similar to results obtained from the microarray analysis. The expression of the *appB* gene was down-regulated at 0*g** but was enhanced at the 2*g** position compared with control by approximately 2-fold. Importantly, no differences in level of expression of these cytochromes were found between the 1*g** and 1*g* static samples, indicating that their expression was not influenced by the magnetic field, but rather by differences in oxygen availability under the different test conditions.

One might speculate that the increase in oxygen availability in the levitated (0*g**) sample may be due to the observed reduction of the rate of sedimentation. This allows bacteria to remain closer to the surface where the liquid is enriched by oxygen diffusing across the air-liquid interface. Whilst this is a plausible hypothesis, we also investigated whether previous studies of magnetically-induced convection in water could be relevant (Hirota 2000, Kishioka 2000, Iwasaka 2003, Peng 2004). Molecular oxygen is paramagnetic and is attracted to a magnetic field: liquid or gaseous oxygen above the solenoid is pulled down towards the center of the solenoid, where the field is largest. This force enhances the buoyancy of objects immersed in the magnetized fluid (Catherall 2003). O_2, dissolved in the liquid culture medium, is similarly attracted by the magnetic field. Since it is consumed by the bacteria and replaced by diffusion across the liquid-air interface, an O_2 concentration gradient results, producing a corresponding gradient in the paramagnetic force density, which can give rise to convection analogous to thermally driven convection. By defining an *effective* liquid density ρ^*, such that the net (magnetic plus gravitational) force on a volume

V of the liquid in the magnetic field can be written as $F = (\chi VBB'/\mu_0 - \rho Vg) = -\rho^* Vg$, we can use existing theory on Rayleigh-Bénard convection to provide an insight into the present problem; ρ and χ are the liquid density (approximately the same as water) and volume magnetic susceptibility, respectively. Since χ depends on the concentration C (molecules per m^3) of dissolved oxygen in the liquid, $\chi = \chi_w + \gamma C$, where $\gamma = 7\times10^{-32}$ m^3, the effective density depends on C. In the $0g^*$ position, the ρ^* of the O_2-rich liquid at the surface is greater than that of the O_2-poor region below. To estimate the value of BB' required to induce convection, we assume for the moment that the bacteria lie in a layer at the bottom of the vessel, so that C decreases linearly from $C_0 \approx 2\times10^{23}$ molecules per m^3 at the liquid-air interface (Benson 1980) to $C = 0$ at the container bottom. We can define a Rayleigh number for this configuration, in analogy with the thermal convection problem (Faber)*,

$$Ra^* = \frac{\alpha g C_0 h^3}{D\nu}$$

Here $h \sim 1$cm is the liquid depth, $D \sim 2\times10^{-9}$ m^2s^{-1} is the diffusivity of O_2 molecules in the medium [approximately the same as that in water (Wilke 1955)], $\nu \sim 1\times10^{-6}$ m^2s^{-1} is the kinematic viscosity of the medium, and α is the fractional change of ρ^* with C,

$$\alpha = -\frac{1}{\rho^*}\left(\frac{\partial \rho^*}{\partial C}\right)_{T,P,(BB')} = \gamma\left(\chi_w + \frac{\rho_w \mu_0 g}{BB'}\right)^{-1} \quad .$$

The fluid is unstable to Rayleigh-Bénard convection (RBC) for $Ra^* > \sim 2000$ (Faber 1995). Hence, we require $BB' > \sim 0.5 T^2 m^{-1}$ for RBC. In our experiments, the bacteria are distributed throughout the liquid, rather than in a layer at the bottom (*E. coli* are also motile). In this case, the theory of RBC cannot be applied directly to the problem. Nevertheless, since $BB' \sim 1500 T^2 m^{-1}$ within the $0g^*$ culture, i.e. much larger than the $0.5 T^2 m^{-1}$ required for RBC in the model case, the Rayleigh-Bénard analysis suggests that convection is likely to occur in our experiments. We note that the culture at $2g^*$ is stable against this type of convection since the paramagnetic force on the O_2 pulls *upward* in this location.

To test experimentally for convection, we performed growth experiments on *E. coli* including the redox dye resazurin. This blue, water-soluble, diamagnetic dye is reduced, irreversibly, to the pink dye resorufin by reactions associated with bacterial respiration (Guerin 2001).

Resorufin can itself be further reduced to the colorless hydroresorufin by the same processes. However, the second reaction is reversible by O_2 (Guerin 2001). Figure 4 shows cultures containing the dye in the 0*g** and 2*g** positions, and in a control sample (1*g*) outside the magnet. The photographs were obtained *in situ*, 6 h after introduction of the dye. Unlike the experiment performed to measure growth, where samples were mixed prior to sampling, these static cultures were left undisturbed. Just after the dye was introduced, all samples had a uniform blue color, but turned pink after approximately 2 h due to bacterial aerobic respiration. The pink color of the 1*g* control sample faded to colorless after a further 1-2 h, as the dissolved O_2 was depleted and the resorufin was further reduced. However, close to the air-liquid interface, the liquid remained pink due to O_2 diffusion across the interface, which prevented the reduction of resorufin to hydroresorufin. In contrast, the color of the sample in the 0*g** position did not fade to colorless, remaining bright pink (including in the region at the bottom of the container), except for the appearance of two paler oval-shaped areas. Comparison with the control sample suggests that within these pale ovals, the O_2 concentration must be lower than in the rest of the fluid. We also note that the oval shapes of these regions are reminiscent of the shape of stagnant regions in thermal convection cells (Faber 1995). These two observations suggest that the concentration of dissolved O_2 *outside* the oval regions is increased by convective transport of O_2 from the relatively O_2-rich surface-liquid to the rest of the sample. The fluid within the ovals stagnates, as is typical in a convection cell, and therefore O_2 levels in these regions are depleted by bacterial respiration, allowing resorufin to be reduced to its colorless form. Note the curvature of the meniscus is largest for the 0*g** sample and smallest for the 2*g** sample (Panel B), consistent with a paramagnetic force acting on the O_2-rich surface layer, pulling up the surface of the 2*g** sample (toward the top of the container), and pushing down the 0*g** sample surface (toward the bottom of the container). Since the paramagnetic force on the O_2 in the 2g* sample acts upward, we expect these samples to be stable against paramagnetic O_2 convection. This is evident from the well-defined pink layer at the top of this container.

A natural question to ask at this point is whether the sedimentation itself is inhibited by the paramagnetic convective stirring, rather than by diamagnetic levitation. Since we observe an *increase* in the rate of sedimentation in the 2g* position, this demonstrates that the diamagnetic force on the liquid and the cells does indeed have an effect on sedimentation, since the liquid in this position is stable against the paramagnetically-induced convection discussed above. However, we must conclude that the convective-stirring has a significant

effect on the availability of O_2 to the bacteria, since the convective flow transports O_2 from the O_2 rich surface through the bulk of the liquid.

Conclusion

From our experimental data, we attribute the increase in bacterial growth rate and higher final cell density in the 0g* samples to enhanced oxygen availability. The effect becomes enhanced at high cell density when the respiration of the bacteria rapidly depletes oxygen levels. This explanation is supported by the observations that (i) the 0*g** sample supplemented with PFC behaves as a uniformly aerated culture and (ii) the anaerobic adaptation genes were more strongly induced in the 1*g** and 2*g** cultures, confirming that they were experiencing oxygen depletion. We have shown that the diamagnetic force can affect the sedimentation rate of a bacterial culture. We have also demonstrated that the gradient magnetic field has a significant effect on the transport of O_2 in liquid cultures: the consumption of O_2 by the living cells and its replenishment by O_2 diffusing across the liquid-air interface can generate convection in the magnetic field, similar to the thermal, Rayleigh-Benard convection process. It is likely that the enhanced availability of O_2 is due to this latter effect. Diamagnetic levitation has the potential to be a powerful technique to study the effects of weightlessness on biological cells, to complement existing Earth-based techniques such as clinorotation and random positioning. However, for diamagnetic levitation to be a useful model of the weightless space environment, where convective transport is absent, paramagnetically-driven convection of O_2 must be prevented. One possibility is to perform experiments on *anerobically* metabolising organisms, or in non-liquid cultures (Beuls et al, 2009).

Materials and Methods

Bacterial cultures. *Escherichia coli* K12 MG1655 and *Staphylococcus epidermidis* NCTC11047 were grown in Nutrient Broth (NB; Oxoid, UK). Gfp^+ bacteria were *E. coli* TOPO(pSB2999) [$P_{rpsJB.subitilis}$::*gfp* in pDEST R4-R3; P.J. Hill, University of Nottingham] which were grown in NB supplemented with Ampicillin (50 $\mu g ml^{-1}$). All cultures were grown at 37 °C aerated by shaking at 150 rpm.

Experimental levitation magnet system. The superconducting solenoid has a 50 mm-diameter vertical bore with an ambient temperature of 12-16 ºC, open to the laboratory at both ends (Fig.S2). A closed-cycle coolant system allows the magnet to run at high magnetic field on time scales of the order of several months. The temperature-controlled chamber consists of an acrylic tube (length 60 cm, internal diameter 44 mm), inserted into the magnet bore, containing three specimen tubes (25mm internal diameter, 25ml capacity), one at each of the 0*g**, 1*g** and 2*g** positions (Fig. S3). The 1*g** position is located at the center of the coil; the 0*g** and 2*g** specimens are located 80mm above and below the 1*g** position, respectively. A constant mean temperature in the bore was maintained, with variation <0.1^{o}C, by temperature-regulated air flow with feedback control. The temperature of each specimen was monitored by a thermocouple in contact with each sample tube. The difference in temperature between the samples was <0.1^{o}C. The effect of magnetic field up to 17 T on the thermocouples was negligible.

Growth Experiments. Cultures were inoculated into fresh NB at an OD_{600nm} = 0.05. The different containers and culture medium volumes used are summarized in Table S1. Samples were exposed to 0*g**, 1*g** or 2*g** for varying periods of time, in the dark at 37 ± 0.2ºC. Each sample was removed from the magnet, mixed, and its cell numbers determined at approximately 1 h intervals to determine growth rate and lag time. Cell number was determined by viable count or by optical density (OD_{600nm}). Resazurin was used at a final concentration of 67 mg ml^{-1} and samples were placed in 2 ml spectrophotometer cuvettes and incubated at 0*g**, 1*g**, 2*g** and 1*g* at 24°C; the lower temperature slowed bacterial growth to allow changes within the fluid to be visualized more easily.

Perfluorocarbon (PFC). Perfluorodecalin (Flutec® PP6) liquid was oxygenated for 20 min with 100% oxygen and dispensed as 4 ml aliquots in sample tubes. For growth experiments, 4 ml of bacterial suspension was overlaid on the PFC and samples exposed to altered gravity in the magnet for 16 h. The position of the sample in the magnet bore was altered to compensate for the raised height of the growth medium due to the presence of the PFC layer in the bottom of the tube. Data were analyzed using the One-way ANOVA and Tukey's pair-wise comparisons post hoc analysis with a 95% confidence interval, using SPSS software.

Microarray analysis. Samples were exposed to each test condition and cells harvested in the mid-exponential phase of growth and 4 independent replicates of each experiment were

performed. Total RNA were extracted and labeled using the protocol outlined in MessageAmp™ II-Bacteria. RNA (700 ng) was labeled with 5-(3-aminoallyl)-UTP. Samples (5µg) of RNA were labeled with Cy5 using NHS-ester reactive dye packs and purified using RNeasy MinElute columns. The DNA reference samples (1µg) were labeled using the Invitrogen 'BioPrime DNA labeling System', with Cy3-dCTP. Agilent MG1655 microarray slides were hybridized at 65°C for 17 h and scanned at 5 µm resolution using the extended dynamic range (Hi 100%, Low 10%). Data were analyzed using Agilent Feature Extraction software and imported into the GeneSpring GX package, normalized per chip to 50% of signal and genes whose normalized expression levels changed 2-fold or more were identified by applying a t-test ($p = 0.05$). Differentially transcribed genes were divided into functional groups using COG and KEGG. A complete analysis of genes involved in oxidative phosporylation pathway with a significantly different level of expression is presented in Table S2.

Real-Time RT-PCR. All qRT-PCR experiments were performed in triplicate on RNA used for microarray analysis and cDNA was synthesized from 2 µg RNA. Custom TaqMan assays for *cyoA, appB* and *envZ* genes were used (Table S3). The thermal profile employed was 50 °C for 2 min, 95 °C for 10 min, and 40 cycles of 95°C for 15 s, 60°C for 1 min. Average C_T values and standard deviation were calculated for the 3 replicates. $\Delta\Delta C_T$ was calculated by the difference between ΔC_T of test samples (0*g**, 1*g**, 2*g** and 1*g* aerated) and control sample (1*g* static).

Footnote. *We emphasize that this number (*Ra**) is not the same as the "magnetic Rayleigh number." The latter is used to characterize convection driven by temperature-induced changes in fluid magnetization, whereas in the present problem, the O_2 concentration gradient is responsible for convection, not the temperature, which is uniform throughout the liquid.

Author contributions. C.E.D., O.L., R.J.A.H. and P.A. performed experiments; C.E.D., O.L., R.J.A.H., P.A., M.R.D., L.E. and C.E.D.R. designed experiments; C.E.D., O.L., C.E.D.R. and R.J.A.H. analyzed data; and C.E.D., O.L., R.J.A.H., L.E. and C.E.D.R. wrote the paper.

Acknowledgements. We thank the technical staff in the School of Physics, especially D. A. Holt, P. Smith, S. R. Booth, S. Nankervis and I. Taylor, for assistance in constructing the temperature-controlled chamber and *in situ* imaging hardware, and P. J. Hill for supplying the GFP bacteria. This work was supported by a Basic Technology Grant from EPSRC, UK.

References

Atlung T, Knudsen K, Heerfordt L, Brøndsted L (1997) Effects of sigma(S) and the transcriptional activator AppY on induction of the *Escherichia coli hya* and *cbdAB-appA* operons in response to carbon and phosphate starvation. *J Bacteriol* 179:2141–2146.

Babbick M, Dijkstra C, Larkin OJ, Anthony P, Davey MR, Power JB, Lowe KC, Cogoli-Greuter M, Hampp R (2007) Expression of transcription factors after short term exposure of *Arabidopsis thaliana* cell cultures to hypergravity and simulated microgravity (2-D/3-D clinorotation, magnetic levitation). *Adv Space Res* 39:1182-1189.

Beaugnon E, Fabregue D, Billy D, Nappa J, Tournier R (2001) Dynamics of magnetically levitated droplets. *Physica B* 294:715-720.

Beaugnon E, Tournier R (1991) Levitation of Water and Organic-Substances in High Static Magnetic-Fields. *J Phys III* 1:1423-1428.

Benson BB, Krause, Jr. D (1980) The concentration and isotopic fractionation of gases dissolved in freshwater in equilibrium with the atmosphere. 1. Oxygen. *Limnol Oceanogr* 25:662-671.

Berry MV, Geim AK (1997) Of flying frogs and levitrons. *Eur J Phys* 18:307-313.

Beuls E, Van Houdt R, Leys N, Dijkstra CE, Larkin OJ, Mahillon J (2009) Bacillus thuringiensis Conjugation in Simulated Microgravity. Astrobiology 9:797

Bouloc P, D'Ari R (1991) *Escherichia coli* metabolism in space. *J Gen Microbiol* 137:2839-2843.

Catherall AT, Eaves L, King PJ, Booth SR (2003) Magnetic levitation: Floating gold in cryogenic oxygen. *Nature* 422:579.

Catherall AT, Lopez-Alcaraz P, Benedict KA, King PJ, Eaves L (2005) Cryogenically enhanced magneto-Archimedes levitation. *New J Phys* 7:118-128.

Cogoli A (2006) in *Fundamentals of Space Biology: Research on Cells, Animals, and Plants in Space, Space Technology Library, Vol. 18*, eds Clément G, Slenzka K (Microcosm Press, El Segundo, CA & Springer NY), pp 121-170.

Coleman CB, Gonzalez-Villalobos RA, Allen PL, Johanson K, Guevorkian K, Valles JM, Hammond TG (2007) Diamagnetic levitation changes growth, cell cycle, and gene expression of *Saccharomyces cerevisiae*. *Biotechnol Bioeng* 98:854-863.

Cotter PA, Gunsalus RP (1992) Contribution of the *fnr* and *arcA* gene-products in coordinate regulation of cytochrome-o and cytochrome-d oxidase (*cyoABCDE* and *cydAB*) genes in *Escherichia coli*. *FEMS Microbiol Lett* 91:31–36.

Denegre JM, Valles JM, Jr., Lin K, Jordan WB, Mowry KL (1998) Cleavage planes in frog eggs are altered by strong magnetic fields. *Proc Natl Acad Sci USA* 95:14729-14732.

Faber TE (1995) Fluid Dynamics for Physicists, Cambridge University Press.

Gasset G, Tixador R, Eche B, Lapchine L, Moatti N, Toorop P, Woldringh C (1994) Growth and division of *Escherichia coli* under microgravity conditions. *Res Microbiol* 145:111-120.

Guerin TF, Mondido M, McClenn B, Peasley B (2001) Application of resazurin for estimating abundance of contaminant-degrading organisms. *Lett Appl Microbiol* 32:340.

Guevorkian K, Valles JM (2006) Swimming *Paramecium* in magnetically simulated enhanced, reduced, and inverted gravity environments. *Proc Nat Acad Sci USA* 103:13051-13056.

Hill RJA, Sedman VL, Allen S, Williams P, Paoli M, Adler-Abramovich L, Gazit E, Eaves L, Tendler SJB (2007) Alignment of Aromatic Peptide Tubes in Strong Magnetic Fields. *Adv Mat* 19:4474-4479.

Hill RJA, Eaves L (2008) Nonaxisymmetric Shapes of a Magnetically Levitated and Spinning Water Droplet. *Phys Rev Lett* 101:234501-4.

Hirota N, Ikezoe Y, Uetake H, Nakagawa J, Kitazawa K (2000) Magnetic Field Effect on the Kinetics of Oxygen Dissolution into Water. *Materials Transactions, JIM* 41:976-80.

Iwasaka M, Yamamoto K, Ando J, Ueno S (2003) Verification of magnetic field gradient effects on medium convection and cell adhesion. *J Appl Phys* 93:6715.

Kacena MA, Manfredi B, Todd P (1999a) Effects of space flight and mixing on bacterial growth in low volume cultures. *Microgravity Sci Technol* 12:74-77.

Kacena MA, Merrell GA, Manfredi B, Smith EE, Klaus DM, Todd P (1999b) Bacterial growth in space flight: logistic growth curve parameters for *Escherichia coli* and *Bacillus subtilis*. *Appl Microbiol Biotechnol* 51:229-234.

Kacena MA, Leonard PE, Todd P, Luttges MW (1997) Low gravity and inertial effects on the growth of *E. coli* and *B. subtilis* in semi-solid media. *Aviat Space Environ Med* 68:1104-1108.

Kishioka S, Yamada A, Aogaki R (2000) Analysis of gas dissociation rate into liquid phase under magnetic field gradient. *Phys Chem Chem Phys* 2:4179-83.

Klaus D, Simske S, Todd P, Stodieck L (1997) Investigation of space flight effects on Escherichia coli and a proposed model of underlying physical mechanisms. *Microbiol* 143:449-455.

Kubitschek HE (1986) Increase in cell mass during the division cycle of *E. coli* B/rA. *J Bacteriol* 168:613-8.

Lynch SV, Brodie EL, Matin A (2004) Role and regulation of sigma(s) in general resistance conferred by low-shear simulated microgravity in *Escherichia coli*. *J Bacteriol* 186:8207-8212.

Nickerson CA, Ott CM, Wilson JW, Ramamurthy R, Pierson DL (2004) Microbial responses to microgravity and other low-shear environments. *Microbiol Mol Biol R* 68:345-361.

Peng ZM, Wang J, Huang YJ, Chen QW (2004) Magnetic field-induced increasing of the reaction rates controlled by the diffusion of paramagnetic gases. *Chem Eng Technol* 27:1273.

Qian A, S Di, Gao X, Zhang W, Tian Z, Li J, Hu L, Yang P, Yin D, Shang P (2009) cDNA microarray reveals the alterations of cytoskeleton-related genes in osteoblast under high magneto-gravitational environment. *Acta Biochim Biophys Sin* 41:561.

Simon MD, Geim AK (2000) Diamagnetic levitation: Flying frogs and floating magnets. *J Appl Phys* 87:6200-6204.

Steiner U, Ulrich T (1989) Magnetic field effects in chemical kinetics and related phenomena, *Chem Rev* 89: 51-147, and references cited therein.

Tanimoto Y, Fujiwara M, Sueda M, Inoue K, Akita M (2005) Magnetic levitation of plastic chips: applications for magnetic susceptibility measurement and magnetic separation. *Jpn J App Phys* 44:6801-6803.

Tsui H-CT, Feng G, Winkler ME (1997) Negative regulation of *mutS* and *mutH* repair gene expression by the Hfq and RpoS global regulators of *Escherichia coli* K-12. *J Bacteriol* 179:7476–7487.

van Loon JJWA (2007) in *Biology in Space and Life on Earth. Effects of Spaceflight on Biological Systems*, ed Brinckmann E (Wiley-VCH Verlag CmbH & Co. KGaA, Weinheim), pp 17-32.

Vytvytska O, Jakobsen JS, Balcunaite G, Andersen JS, Baccarini M, von Gabain A (1998) Host factor I, Hfq, binds to *Escherichia coli ompA* mRNA in a growth rate-dependent fashion and regulates its stability. *Proc Natl Acad Sci USA* 95:14118–14123.

Wilke CR, Chang P (1955) Correlation of diffusion coefficients in dilute solutions. *A.I.Ch.E. J.* 1:264-270.

Wilson JW, Ott CM, Honer zu Bentrup K, Ramamurthy R, Quick L, Porwollik S, Cheng P, McClelland M, Tsaprailis G, Radabaugh T, Hunt A, Fernandez D, Richter E, Shah M, Kilcoyne M, Joshi L, Nelman-Gonzalez M, Hing S, Parra M, Dumars P, Norwood K, Bober R, Devich J, Ruggles A, Goulart C, Rupert M, Stodieck L, Stafford P, Catella L, Schurr MJ, Buchanan K, Morici L, McCracken J, Allen P, Baker-Coleman C, Hammond T, Vogel J, Nelson R, Pierson DL, Stefanyshn-Piper HM, Nickerson CA (2007) Space flight alters

bacterial gene expression and virulence and reveals a role for global regulator Hfq. *Proc Natl Acad Sci USA* 104:16299–16304.

Figures

Figure 1. Sedimentation and growth of cultures in the magnet

Samples of *E. coli*(pSB2999) expressing the green fluorescence protein were grown in the magnet at 0*g**, 1*g** and 2*g** statically for 18 h at 37 °C and then visualized under UV illumination.

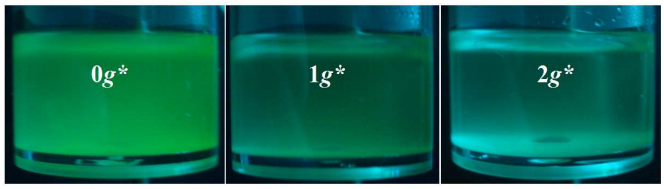

Figure 2. Growth of *E. coli* and *S. epidermidis*

Cultures of *E. coli* (Panel A) and *S. epidermidis* (Panel B) were grown at 37 °C in nutrient broth. They were either exposed to altered effective gravity in the magnet bore [(♦) 0*g**, (■) 1*g**, (▲) 2*g**] or were grown outside the magnet (1*g*) [(○) statically, (◊) aerated]. Samples were collected at hourly intervals in order to determine the cell mass, using OD_{600nm}.

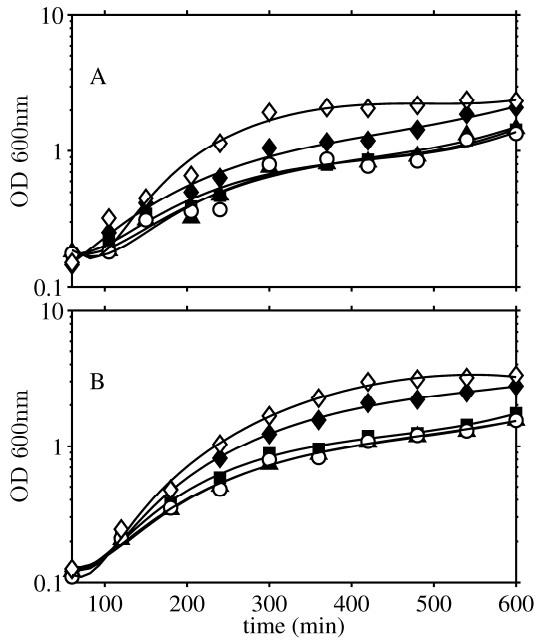

Figure 3. Relationship between final cell mass and liquid-air interface area/sample volume.

Samples were incubated for 18 h in tubes with different dimensions (Table S1). The optical density (OD_{600nm}) after 18 h shows a clear increase with A/V; A is the area of the liquid-air interface and V is the sample volume. Panels A and B: OD of the 0g* sample [OD(0g*)] relative to the OD of the 1g* control sample in the magnet [OD(1g*)] (A) and 1g control outside the magnet [OD(1g)] (B). Panel C: OD of the 1g control. Lines show the least-squares linear fit to the data.

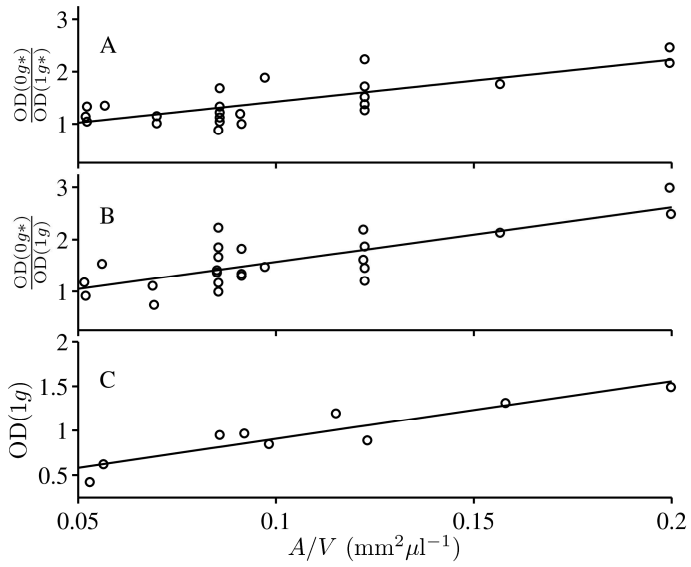

Figure 4. Magnetic convection in a bacterial culture

Static bacterial cultures (*E. coli*) in 10mm x 10mm x 45mm cuvettes, containing resazurin dye. Cuvettes in the 0*g** and 2*g** positions in the magnet, and 1*g* control outside the magnet, photographed *in situ* after 6 h. The dye turns pink in regions where bacteria are undergoing aerobic metabolism but have not become anaerobic, highlighting areas with a relatively high O_2 concentration. Image at top right is a false-color reproduction of the 0*g** image, highlighting the shape of the O_2-depleted regions in blue; their shapes are reminiscent of the shape of thermal convection cells.

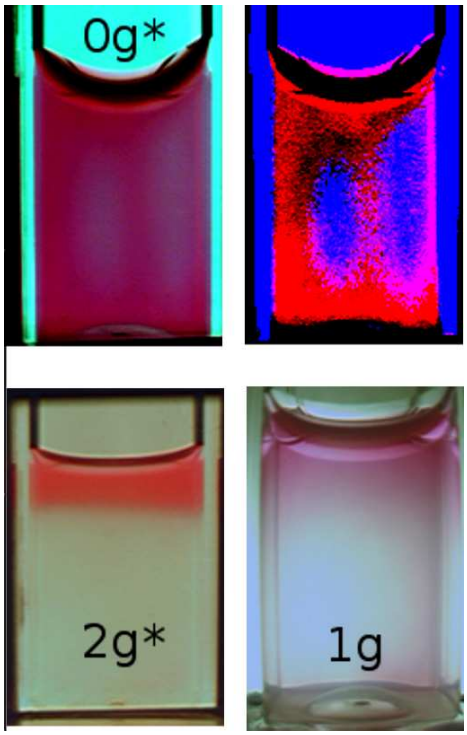

Tables

Table 1(a and b). Effects of culture conditions on cell growth.

Cultures were grown under different test conditions for 18 h at 37 °C in the 0*g**, 1*g** and 2*g** positions. The 1*g* control samples were grown outside the magnet either statically (1*g*) or with shaking (1*g* aerated). Optical density (OD_{600nm}) of samples was determined after 18h. Table 1a; final optical densities of cultures of *E. coli* grown without and with O_2-gassed perfluorodecalin (PFC) layer at the bottom of the culture. Table 1b; ratios of final cell density values of *E. coli* and *S. epidermidis* cultures. Only *E. coli* static cultures were oxygenated from the bottom of the culture by adding O_2-gassed PFC.

a)

Final cell density (OD_{600nm})		
Condition	**Without PFC**	**With PFC**
0*g**	1.9 ± 0.3	2.3 ± 0.1
1*g**	1.4 ± 0.1	1.9 ± 0.1
2*g**	1.3 ± 0.2	1.8 ± 0.1
1*g*	1.3 ± 0.1	1.8 ± 0.1
1*g* aerated	2.4 ± 0.2	n.d.

b)

Test Comparison	*E. coli*	*E. coli* with PFC	*S. epidermidis*
0*g**/ 1*g*	1.73 ± 0.35	1.24 ± 0.05	1.94 ± 0.16
1*g**/ 1*g*	1.09 ± 0.03	1.06 ± 0.07	1.17 ± 0.25
2*g**/ 1*g*	1.04 ± 0.08	1.01 ± 0.02	0.73 ± 0.11
0*g** / 1*g**	1.59 ± 0.29	1.16 ± 0.03	1.53 ± 0.16
0*g** / 1*g* aerated	0.9 ± 0.05	n.d.	0.81 ± 0.02

n.d, not done

Table 2. Microarray analysis of changes in expression of cytochromes and *fnr*

Comparison of significant fold changes in expression for genes involved in cytochrome regulation in *E. coli* K12 MG1655. Samples were exposed to altered effective gravity at 37 °C in the magnet bore (0*g**, 1*g** or 2*g**) or grown outside the magnet (1*g*) either statically or aerated. All samples were harvested at OD_{600nm} = 0.5 for RNA extraction to minimize effects caused by changes in cell population and associated depletion of gases and nutrients. Total RNA was extracted from 4 independent replicates and used for microarray analysis. Data were analyzed using GeneSpring GX 7.3, and normalized against 50% of signal for each independent array and filtered using p-value = 0.05.

Test conditions	Gene	Gene Product	Fold change
0*g* vs. 1*g*****	*cyoA*	cytochrome o ubiquinol oxidase subunit II	2.11
	cyoB	cytochrome o ubiquinol oxidase subunit I	2.34
	appA	phosphoanhydride phosphorylase	0.47
	appC	cytochrome bd-II oxidase, subunit I	0.45
0*g* vs. 2*g*****	*cyoB*	cytochrome o ubiquinol oxidase subunit I	2.98
	appB	cytochrome bd-II oxidase, subunit II	0.33
	appC	cytochrome bd-II oxidase, subunit I	0.2
	Fnr	DNA-binding transcriptional dual regulator, global regulator of anaerobic growth	0.43
0*g* vs. 1*g***	*cyoD*	cytochrome o ubiquinol oxidase subunit IV	2.12
	cyoE	Protoheme IX farnesyltransferase	2.12
	Fnr	DNA-binding transcriptional dual regulator, global regulator of anaerobic growth	0.37
1*g* vs. 1*g* aerated**	*cyoB*	cytochrome o ubiquinol oxidase subunit I	0.42
1*g* vs. 2*g*****	*appB*	cytochrome bd-II oxidase, subunit II	0.47
	appC	cytochrome bd-II oxidase, subunit I	0.4

Table 3. Comparison of qRT-PCR and microarray data for *cyoA* and *appB*

Samples of RNA extracted for the array experiments from 4 independent replicates of cells grown in altered effective gravity at 37°C in the magnet bore (0*g**, 1*g** or 2*g**) or statically outside the magnet (1*g*), were used for qPCR analysis. Cells were recovered from each culture for RNA extraction when OD_{600nm} = 0.5. Details of TaqMan probes and dyes used are provided in Table S3.

	Fold change			
Test conditions	***cyoA***		***appB***	
	Arrays	**qRT-PCR**	**Arrays**	**qRT-PCR**
0*g** /1*g*	1.49*	1.57*	0.69	0.80
1*g**/1*g*	0.71	0.90	0.88	0.92
2*g** /1*g*	0.95	0.80	1.82*	2.20*

* p values < 0.05

Supplementary Information

Figure S1. Calculated effective gravity Γ inside a 25 ml specimen tube in the 0*g** position. The tube is 25mm in diameter and 40mm tall, excluding the top cap (gray rectangle). The magnitude of Γ is shown by contours. The contour labels show the magnitude of the effective gravity as a percentage of 1*g*, i.e. 100Γ/*g*, where g=9.8ms^{-2}. The arrows show the direction of the effective gravity vector **Γ**.

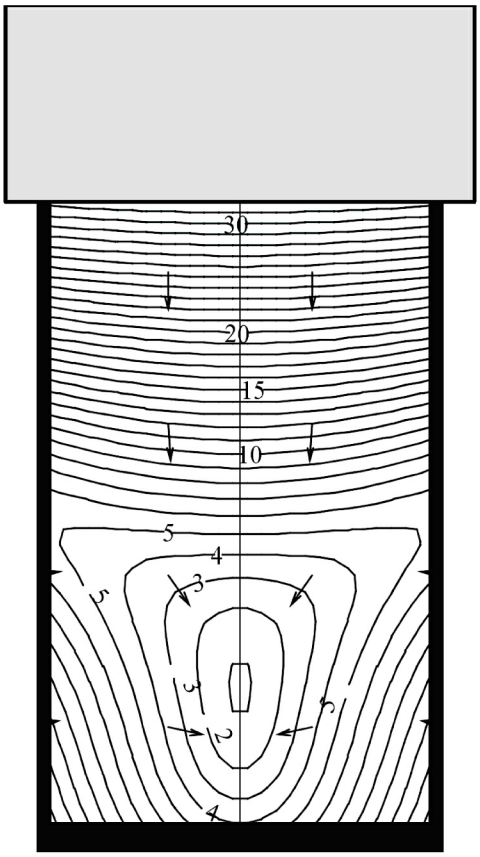

Figure S2. A) Schematic of the cryostat housing the solenoid magnet. The 5cm-diameter bore and the superconducting solenoid are indicated. B) Photograph of the top plate of the cryostat showing the entrance to the bore.

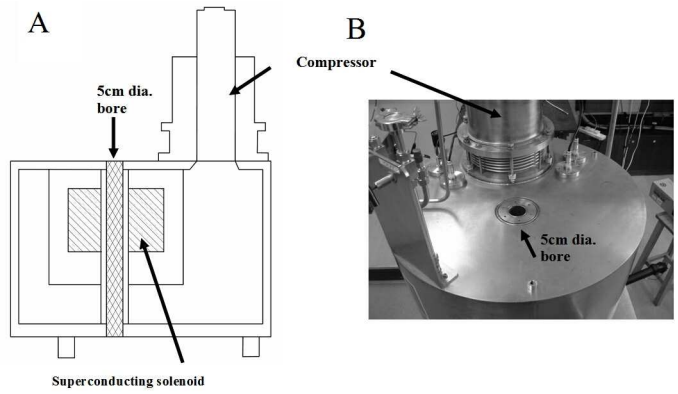

Figure S3. Temperature-regulated chamber containing three specimen tubes. i) frame used to hold specimen tubes in the 0g*, 1g* and 2g* positions within the magnet. Specimen tubes are supported by nylon collars attached to three threaded brass rods. The position of the collars is adjustable. White LED lighting and web cameras, stripped of ferromagnetic components, were installed to obtain images of the samples *in situ*. Thermocouples, connected to a data logger, were installed to monitor the temperature of each sample. ii) frame located within the temperature-regulated chamber; air-flow ports can be seen top and bottom. The air supply is passed through a heat exchange coil immersed in a thermostatically-controlled water bath.

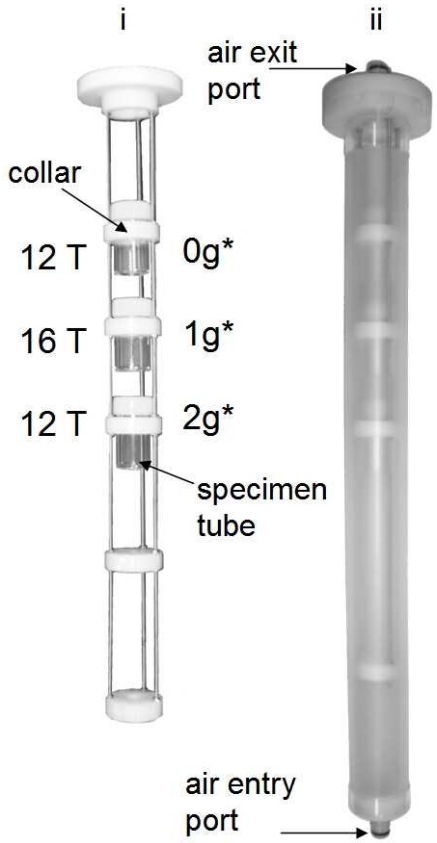

Table S1 Dimensions of the culture vessels used within the magnet bore

Container	Volume (µl)	Surface area vs. Volume ($mm^2 µl^{-1}$)
0.2ml Tubes	100	0.200
	200	0.115
	300	0.085
0.5ml Tubes	200	0.157
	350	0.092
	600	0.056
	700	0.053
25ml Tubes	700	0.698
	4000	0.122
	5000	0.098

Table S2. Comparison of significant fold changes (p < 0.05) in expression for genes involved in cytochrome regulation in *E. coli* K12 MG1655.

Test conditions	Gene	Gene Product	Fold change
0*g vs. 1*g****	*cyoA*	cytochrome o ubiquinol oxidase subunit II	2.11
	cyoB	cytochrome o ubiquinol oxidase subunit I	2.34
	ndh	respiratory NADH dehydrogenase, aerobic respiration	2.41
	appA	phosphoanhydride phosphorylase	0.47
	appC	cytochrome bd-II oxidase, subunit I	0.45
0*g vs. 2*g****	*cyoB*	cytochrome o ubiquinol oxidase subunit I	2.98
	appB	cytochrome bd-II oxidase, subunit II	0.33
	appC	cytochrome bd-II oxidase, subunit I	0.20
	ppa	inorganic pyrophosphatase (phosphorus metabolism)	0.35
	fnr	DNA-binding transcriptional dual regulator, global regulator of anaerobic growth	0.43
0*g vs. 1*g***	*cyoD*	cytochrome o ubiquinol oxidase subunit IV	2.12
	cyoE	protoheme IX farnesyltransferase	2.12
	atpC	F1 sector of membrane-bound ATP synthase, epsilon subunit (ATP synthesis coupled proton transport)	2.10
	fnr	DNA-binding transcriptional dual regulator, global regulator of anaerobic growth	0.37
1g* vs. 1*g* aerated	*cyoB*	cytochrome o ubiquinol oxidase subunit I	0.42
1*g vs. 2*g****	*appB*	cytochrome bd-II oxidase, subunit II	0.47
	appC	cytochrome bd-II oxidase, subunit I	0.40
	ppa	inorganic pyrophosphatase (phosphorus metabolism)	0.34
1*g* vs. 2*g**	*frdC*	fumarate reductase (anaerobic),	0.25
	frdD	fumarate reductase (anaerobic),	0.42
	ppa	inorganic pyrophosphatase (phosphorus metabolism)	0.41
	atpC	F1 sector of membrane-bound ATP synthase, epsilon subunit (ATP synthesis coupled proton transport)	0.47
1g vs. 1*g* aerated	*cyoE*	protoheme IX farnesyltransferase	0.48

To ensure changes seen were due to suspension of cells, changes in expression due to the magnetic field alone (comparison of 1*g** and 1*g* results) were removed from analysis. Samples were exposed to altered effective gravity at 37 ℃ in the magnet bore (0*g**, 1*g** or 2*g**) or grown outside the magnet (1*g*) either statically or aerated. All samples were harvested at OD_{600nm} = 0.5 for RNA extraction to minimize effects caused by changes in cell population and depletion of gases and nutrients. Total RNA was extracted from 4 independent replicates and used for microarray analysis. Data were analyzed using GeneSpring GX 7.3, and normalized against 50% of signal for each independent array and filtered using p-value = 0.05.

Table S3. Primers and probes used for qRT-PCR analysis

Gene	Forward Primer	Reverse Primer
appB	GGAGTATCTCGGCAGCTTCTG	GCTGAGCAATCCGCACAATAAAG
envZ	CCCGGCAGCATTGAAGTGA	CCACCGCGCGTTTGATC
cyoA	CGAGAAGCCCATTACCATCGAA	CCTGTTCCGGGTAGATGAAGAA

Reporter 1 Name	Reporter 1 Dye	Reporter 1 Sequence
APPB-AP1M1	FAM	CTGCTGACGCCATTCC
ENVZ-EN4M2	FAM	ACAGCGGGTGCATTT
CYOA-CO1M2	FAM	CCAGTCCATGGAAACCA